

Relationship between crack size and residual water evaporation during vacuum drying of simulated damaged spent nuclear fuel

Ji Hwan Lim^{a*}, Seung-Hwan Yu^a, Kyoung-Sik Bang^a, Gyung-sun Chae^b, Kyung-Wook Shin^b, Nam-Hee Lee^b

^a*Transportation and Storage R&D Division, Korea Atomic Energy Research Institute, 111 Daedeok-daero 989 beon-gil, Yuseong-gu, Daejeon 34057, Republic of Korea*

^b*SAE-AN Engineering Corporation, #910, 184 Gasan digital 2-ro, Geumcheon-gu, Seoul, 08501, Republic of Korea*

**Corresponding author: jlim@kaeri.re.kr*

***Keywords :** Vacuum drying, Simulated damaged fuel, Dry storage system, Residual water, Crack

1. Introduction

In the industrial application of vacuum drying for damaged nuclear fuel rods, one of the critical variables impacting the drying process is the size of cracks within the rods. These cracks significantly affect the dynamics of residual water evaporation and consequently the efficiency of the vacuum drying process. This study specifically examines how variations in crack size influence the evaporation of residual water in nuclear fuel rods. The initial findings indicate that while the internal pressure behavior does not significantly differ with crack size, larger cracks tend to extend the drying time because of increased expulsion of water during critical evaporation phases. This necessitates a thorough investigation into the influence of crack size on the drying process to optimize protocols for effective moisture removal under varying structural conditions.

Several studies have addressed related aspects of drying spent nuclear fuel, providing valuable insights while also revealing areas requiring further exploration. For instance, Demuth et al. [1] conducted engineering-scale tests to evaluate vacuum and forced helium dehydration (FHD) methods, finding that both were effective in removing bulk water. However, FHD was superior in removing chemisorbed water due to higher drying temperatures. Despite these findings, the study focused more on thermogravimetric analysis of aluminum surrogate plates rather than exploring the effects of crack size on drying efficiency. Similarly, Goode et al. [2] compared vacuum and flowed gas drying methods for small-scale spent nuclear fuel pins, noting that vacuum drying achieved significantly higher drying rates. This study, however, was limited to comparisons of pinholes and stress corrosion cracks, providing limited insight into how varying crack sizes affect drying. Perry et al. [3] conducted engineering-scale tests on aluminum-clad spent nuclear fuel, focusing on understanding and modeling drying conditions. While the study demonstrated the importance of local temperature in removing chemisorbed water, it did not investigate the impacts of crack sizes on overall drying efficacy.

Further research by Eidelpes and Petersen [4] assessed dry storage canister pressures and the potential for forming a flammable atmosphere, focusing on developing bounding pressure models. This work, while critical for safety evaluations, did not delve into the role of crack dimensions during the vacuum drying process. Pulido et al. [5] utilized mass spectrometry to quantify residual water in dry storage canisters, aiming to validate the efficacy of commercial drying procedures. However, this study primarily concentrated on validating drying completeness, without specifically addressing the influence of crack size on residual water dynamics.

The reviewed literature suggests a foundational understanding of drying processes in spent nuclear fuel storage, yet it reveals significant gaps, particularly concerning the role of crack size. This oversight underscores the necessity for detailed research to quantify how different crack sizes influence evaporation rates and residual water removal efficiency. Such an investigation is critical for optimizing drying protocols, ensuring both safety and efficiency in storage systems for damaged nuclear fuel. Understanding these dimensions can yield actionable insights into balancing drying efficiency with material integrity, ultimately contributing to more robust and reliable storage solutions in nuclear fuel management.

2. Experimental Method

2.1 Instrumentation and Apparatus Overview

The conception and development of the vacuum drying apparatus necessitate a profound comprehension of its technical specifications, given the absence of standardized procedural directives for such equipment. Consequently, the design is derived from an in-depth examination of experimental exigencies, objectives, and the scope of the tests [6, 7]. The system is principally engineered to extract residual moisture from irradiated nuclear fuel within spent fuel storage environments, where operational compatibility and structural robustness are paramount. The apparatus is constructed not only to meet the intricate technical demands of nuclear facilities but also to ensure its operational

efficacy under stringent conditions. A pilot-scale unit has been conceived to critically assess the performance of the vacuum drying process, specifically quantifying the residual moisture after the drying cycle and testing its reliability for full-scale application.

In practical terms, the equipment design integrates operational mobility via pre-existing hoisting mechanisms, preventing potential displacement or instability during use. Emission control and management, though less pertinent at the laboratory scale, are of critical concern at full deployment. Gaseous emissions are routed to the plant's HVAC systems, while condensed liquid byproducts are temporarily contained for future treatment and disposal. To ensure minimal exposure to radiation, a centralized control system is incorporated, allowing all system operations to be managed remotely. The apparatus comprises a suite of essential components, including high-performance vacuum pumps for pressure reduction, condensation units for moisture extraction, drainage pathways, and pressure monitoring devices. Residual moisture content is quantitatively assessed via a real-time moisture measurement program, thereby ensuring precision in both operation and data acquisition. The apparatus's modular design allows seamless adaptation to various experimental configurations, with key components—such as vacuum pumps, cold traps, and measurement sensors—meticulously aligned with industry standards and regulatory frameworks, including those delineated in NUREG-2215 and ASTM C1553-16.

2.2 Configuration of Test Specimens

The simulated damaged nuclear fuel rods were fabricated using ZIRLO, a material selected for its comparable properties to those found in real spent nuclear fuel. These rods were dimensioned according to the specifications of the PLUS7 and ACE7 fuel designs, which share identical outer and inner diameters of 9.5mm and 8.357mm, respectively. The rods were truncated to a length of 100mm, after which an endcap was welded to the bottom and an M5-tapped open cap was affixed to the top, providing an access point for controlled introduction of residual water. In order to simulate varying degrees of mechanical degradation, hole-milling was performed at the rod's midsection (50mm from the base), creating cracks of different diameters: 0.3, 0.5, 1.0, and 2.0mm.

2.3 Methodological Framework for Vacuum Drying

The vacuum drying procedure was meticulously conducted using the following steps: Initially, the vacuum pump was selected and connected to the experimental apparatus. After activating the power to initiate system operation, the cold trap temperature was allowed to stabilize below -20°C . The canister lid was

then removed with the aid of a crane, and a rack was positioned within the canister to support the microbalance, upon which the damaged nuclear fuel specimen was placed. The fuel was adjusted so that the cracks became visible through the observation window. A predetermined amount of 2g of residual water was introduced into the fuel rod via syringe, after which the thermocouple was positioned within the water to monitor its temperature. The canister was then sealed, and the measurement system on the connected computer was activated. The moisture measurement program was initiated, and a file name was designated for data storage.

The vacuum pump was subsequently engaged to reduce the internal pressure of the canister to 1.5 torr, which was maintained for a duration of 30 minutes to ensure optimal drying conditions. Once these conditions were met, the moisture measurement program was halted, and the vacuum pump was switched off. Following this, the power to the test equipment was terminated, and the pressure inside the canister was normalized to atmospheric levels. The canister lid was then opened, and any residual water within the test specimen was carefully retrieved for subsequent analysis.

3. Result and Discussion

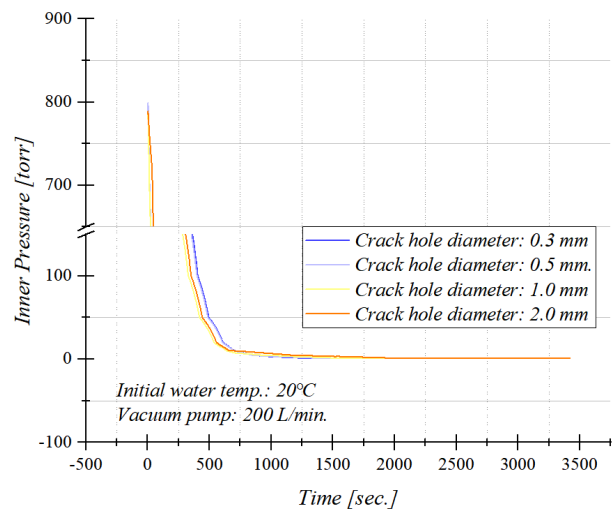


Fig. 1. Effect of Crack Size on Internal Pressure Dynamics Over Time

Figure 1 presents the dynamics of internal pressure fluctuations over time in response to varying crack dimensions—specifically, 0.3mm, 0.5mm, 1.0mm, and 2.0mm—within the framework of an initial water temperature of 20°C and pump action at 200 L/min. Despite the change in crack size, the pressure reduction trajectory within the canister remained largely consistent. Notable differences emerged, however, in the total duration needed to fulfill vacuum drying stipulations, inclusive of the obligatory 30-minute holding interval. The drying durations for each crack

size were recorded as 3255.5, 3391.5, 3572.9, and 4102.1 seconds, respectively, with larger apertures necessitating extended drying.

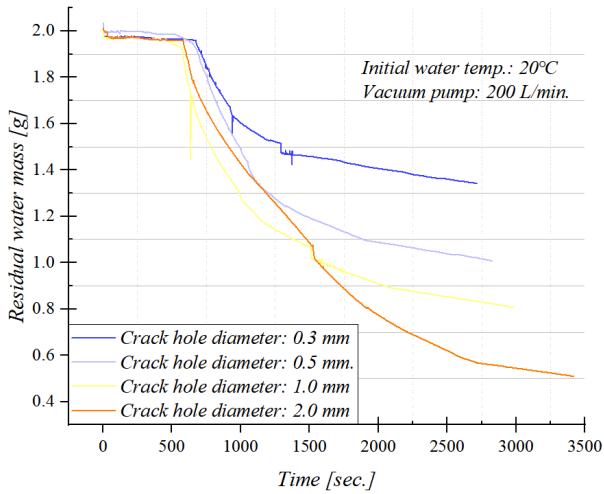


Fig. 2. Effect of Crack Size on Temporal Residual Water Mass Dynamics

Figure 2 delves into how crack dimensions directly affect the temporal progression of residual water removal. Predominantly driven by enhanced evaporation during the critical phase change, the time to reach such a boundary remained uniform across different crack sizes, with the onset of notable mass reduction consistently occurring around 750 seconds. Yet, the overall drying time and the quantity of water dispelled varied with crack size. Specifically, a 2.0mm crack achieved a substantially reduced water mass to 0.501g, whereas a 1.0mm crack left a larger 1.342g within the rod. Data detailing this trend across various crack sizes—0.3mm, 0.5mm, 1.0mm, and 2.0mm—confirm the pattern of diminished residual water as crack size increased.

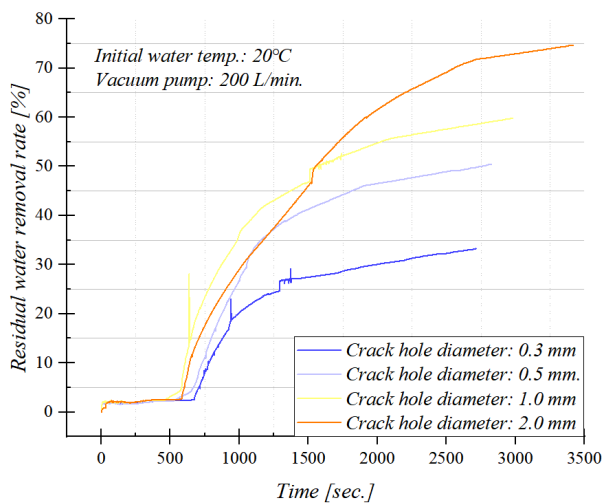


Fig. 3. Influence of Crack Size on Removal Rate of Residual Moisture

In Figure 3, the removal ratio over time provides a visual exposition of the correlation between crack dimensions and water expulsion efficacy. Larger apertures prolong drying phases while facilitating the expulsion of more substantial water quantities. For instance, the removal success rate for a 0.3mm crack was 33.27%, while a 2.0mm aperture exceeded this, achieving a rate of 75.09%. The data underscore that while larger cracks improve evaporation efficiency during the phase change transition, they introduce trade-offs like extended drying times and challenges achieving ultra-high vacuum due to secondary water expulsion. The direct role of aperture size in water removal is clearly proportional, with larger cracks leading to better removal ratios across various conditions. Conversely, Figure 3 reveals an inverse relationship between crack size and failure rate, indicating that smaller cracks generally correlate with higher failure in water removal. Notably, even with a 2.0mm crack and robust suction at 600 L/min, about 25% of the water remained inside, highlighting opportunities for refining drying methodologies to enhance efficiency.

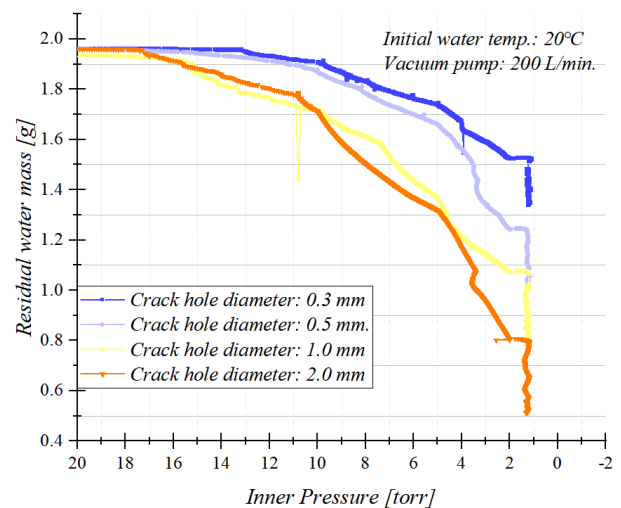


Fig. 4. Pressure-Induced Variation in Mass Reduction and Crack Size Impact

Figure 4 shows the unique relationship between pressure changes and water removal across different aperture sizes. Depicted within a pressure spectrum from 15 to 20 torr, major reduction in water mass is vivid once this critical pressure range is entered. Larger cracks exhibit a more pronounced mass decline during this evaporation-boosting phase. Delving deeper into this phase, it becomes apparent that the influence of crack size on evaporation intensifies as pressure lowers. An anomaly noted within the 100 L/min scenario, where a 1.0mm crack outperformed a 2.0mm crack in removal success, stemming likely from peculiar bulk water dynamics during discharge, exemplifies the nuanced interplay of structural variables in water expulsion dynamics.

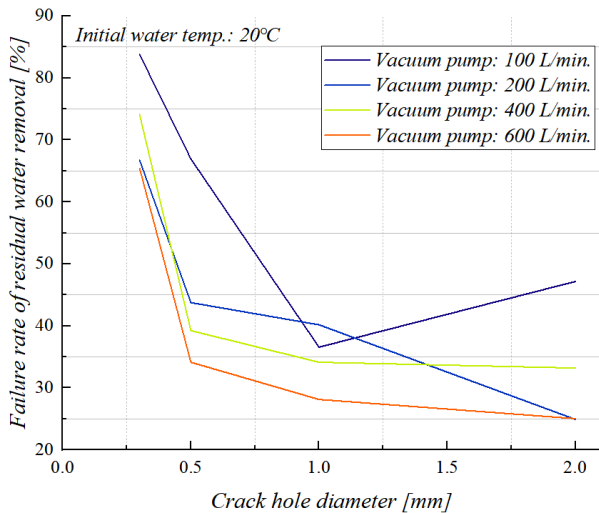


Fig. 5. Comprehensive Evaluation of Crack Size on Moisture Removal Failures

Finally, Figure 5 documents the failure rate under varying crack sizes, reinforcing that even substantial apertures like 2.0mm fail to ensure complete residual water removal. Enhanced insights establish a fertile ground for further exploration, underscoring a manifest need for innovative drying solutions aimed at efficiently handling residual moisture in damaged nuclear fuel rods.

In conclusion, while augmenting crack size bolsters residual water expulsion, it does not assure total drying. Detailed analyses reveal vital thermodynamic exchanges involving crack geometry and phase transition dynamics that underpin evaporation processes. The partial efficacy of even substantial apertures like 2.0mm implies explorations beyond structural modifications are essential. These results lay the groundwork for advancing drying process efficiency and reliability for spent nuclear fuel rods in industrial settings.

4. Conclusions

This investigation explored the influence of crack morphology on the desorption dynamics of residual water in compromised nuclear fuel rods during vacuum drying. The results substantiate that an augmentation in crack aperture substantially enhances the efficacy of water expulsion, establishing a proportional relationship between crack size and the volume of water evacuated. This phenomenon is attributable to the expedited evaporation at the phase transition interface, where larger fissures facilitate a more rapid equilibration of internal and external pressures, thereby accelerating the desorption process. However, these advantages are accompanied by notable trade-offs. While larger cracks promote a more efficient removal of water, they also necessitate extended drying durations and introduce complexities in achieving ultra-high vacuum states, primarily due to secondary evaporation from water deposited on the canister's base. Interestingly, even for

the maximum crack dimension of 2.0 mm, a considerable fraction (up to 25%) of the residual water remained retained, especially under reduced pump suction capacities.

The study further elucidates that the critical threshold for initiating enhanced evaporation occurs within a narrow pressure range of 15 to 20 torr, with larger cracks enabling a more rapid attainment of this zone. Despite the observed improvements in efficiency for larger fissures, the results underscore the necessity for further advancements in vacuum drying methodologies to mitigate the challenges of incomplete water removal. These findings underscore the pivotal role of crack geometry in optimizing drying protocols and provide a foundational framework for subsequent investigations into the refinement of vacuum drying techniques for damaged nuclear fuel rods. More attention and additional research are required for the transportation and storage of spent nuclear fuel in South Korea [8].

Acknowledgements

This work was supported by the Institute for Korea Spent Nuclear Fuel (iKSNF) and National Research Foundation of Korea (NRF) grant funded by the Korea government (Ministry of Science and ICT, MSIT) (No. 2021M2E1A1085226).

REFERENCES

- [1] Demuth, R. J., D'Entremont, A. L., Smith, R., Sindelar, R. L., Knight, T. W., 2024, "Drying and Analysis of Aluminum (Oxy) hydroxide Films for Dry Storage of Aluminum-Clad Spent Nuclear Fuels," Nuclear Technology, Vol. 210, No. 11, pp. 2187-2203.
- [2] Goode, J. B., Hambley, D. I., Hanson, B. C., 2019, "A benchtop comparison of drying methods relevant to failed spent nuclear fuel," Progress in Nuclear Energy, Vol. 115, pp. 120-125.
- [3] Perry, J., Demuth, R., Cooper, N., Knight, T., Parisi, N., Stafford, G., Smith, R. E., 2021, "Engineering Scale Drying of Aluminum-Clad Spent Nuclear Fuel: Experiment Report," Idaho National Laboratory (INL), Report No. INL/EXT-21-62416-Rev000, Idaho Falls, ID (United States).
- [4] Eidelpes, E. F., Petersen, G. M., 2024, "Bounding Pressure and Flammability Evaluations of Aluminum-Clad Spent Nuclear Fuel Department of Energy Standard Canisters," Idaho National Laboratory (INL), Report No. INL/CON-23-75103-Rev001, Idaho Falls, ID (United States).
- [5] Pulido, R. J., Taconi, A. M., Williams, R. W., Baigas, B. T., Durbin, S. G., 2024, "Quantification of Residual Water in Spent Fuel Dry Storage Canisters Using Mass Spectrometry," Sandia National Laboratories (SNL-NM), Report No. SAND-2024-03859R, Albuquerque, NM (United States).
- [6] Lim, J. H., Bang, K. S., Shin, K. W., Lee, N. H., Yu, S. H., 2025, "Comprehensive evaluation of residual water based on vacuum drying methods," Nuclear Engineering and Technology, 103430.
- [7] Lim, J. H., Bang, K. S., Shin, K. W., Lee, N. H., Yu, S. H., 2024, "Accuracy and error in measuring residual water mass quantity in spent nuclear fuel canisters after vacuum drying,"

In Proc. Trans. Korean Nuclear Society Autumn Meeting, pp.
1-6.
[8] Choi, S., Lim, J., "A Review on Sabotage Against
Transportation of Spent Nuclear Fuel", Proceedings of the
Korean Nuclear Society Autumn Meeting, 1-4, Oct., 2016.